Synaptic Transmission in PNS: the **Neuromuscular Junction**

1. The Synaptogenesis
2. **The Synaptic Transmission at NMJ**
3. The Safety Factor
4. Myasthenic Syndromes
5. The Tripartite Synapse

First animal model: Squid

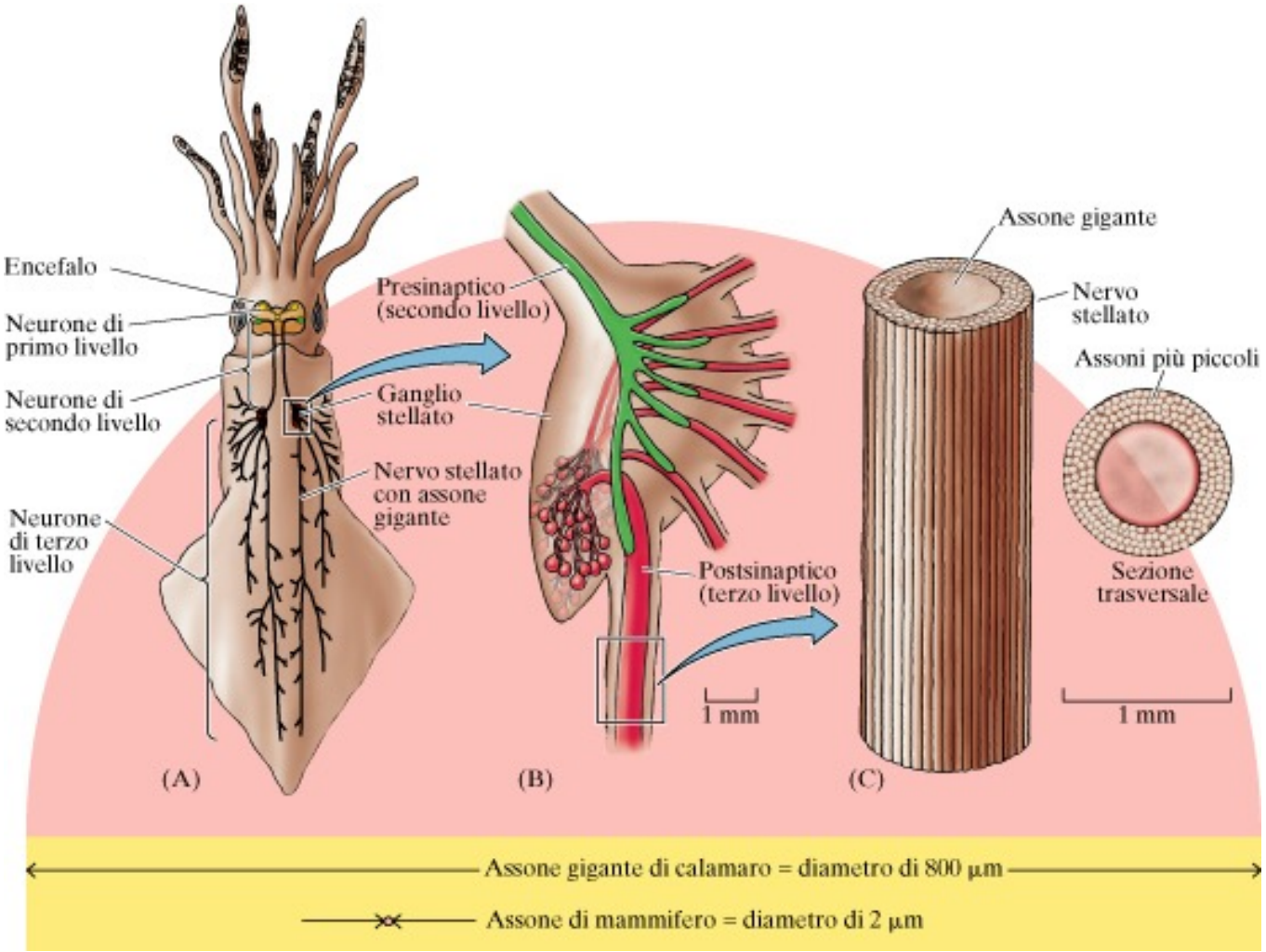

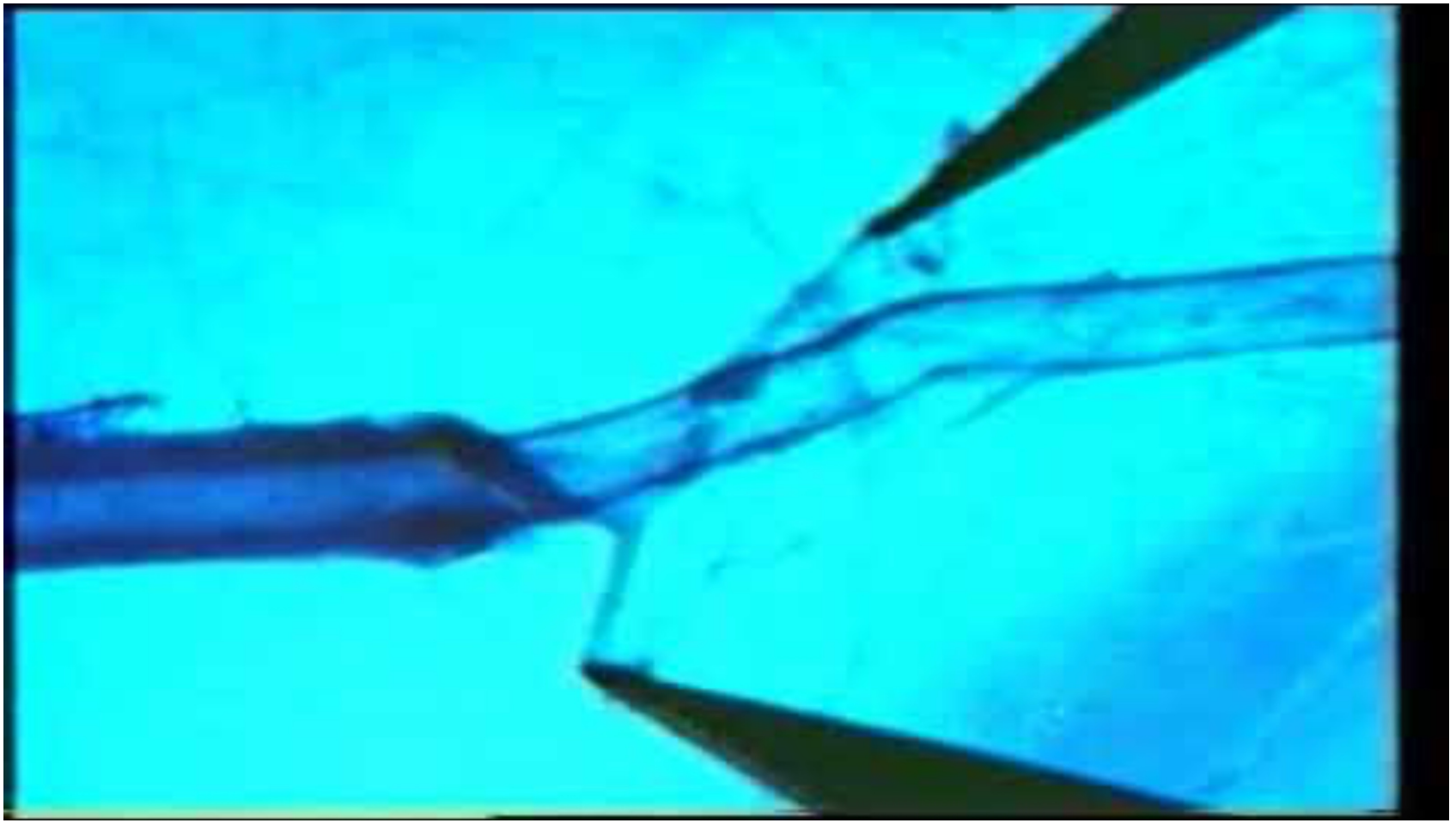

https://www.youtube.com/watch?v=CXCGqwdtJ78

The first direct recorded action potential by Hodgkin and Huxley (squid giant axon)

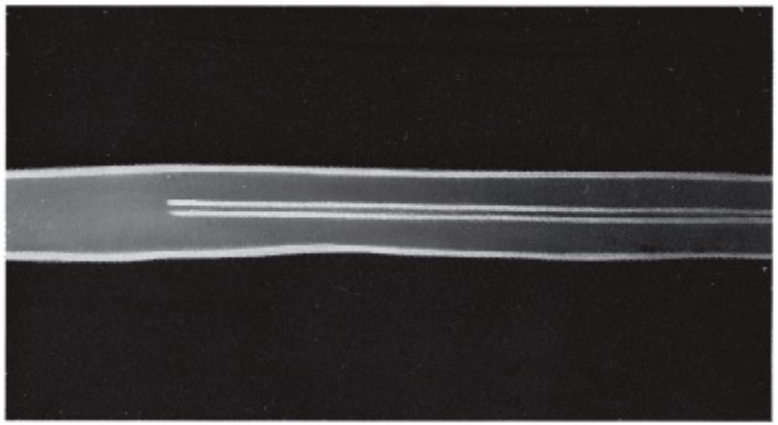

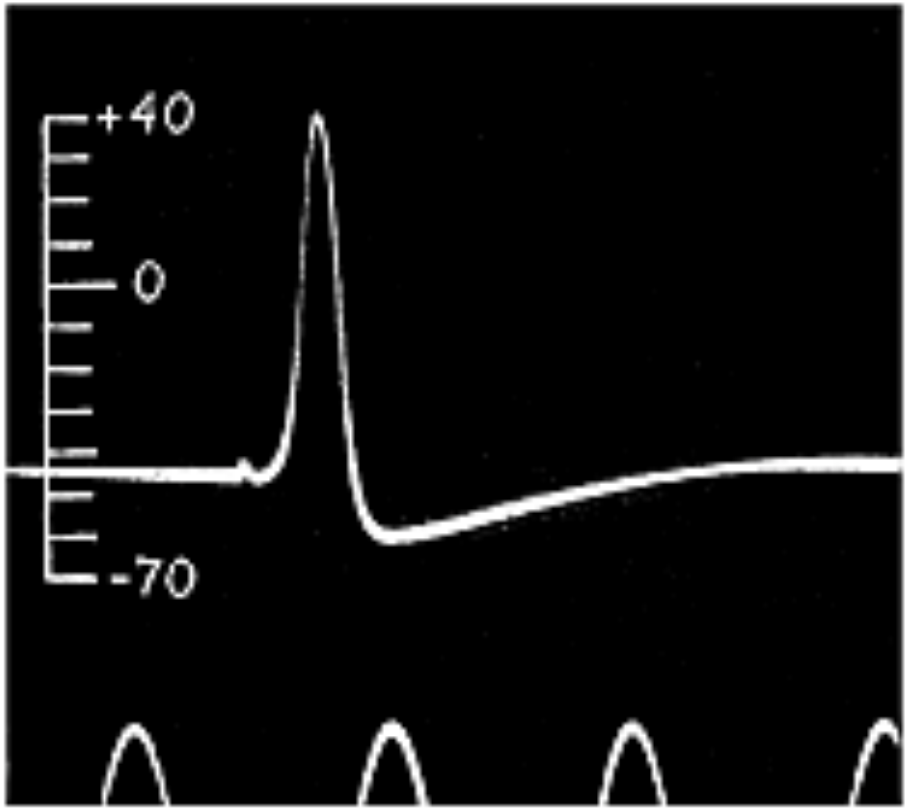

The stellate ganglion of the squid: a model for studying the chemical synapse

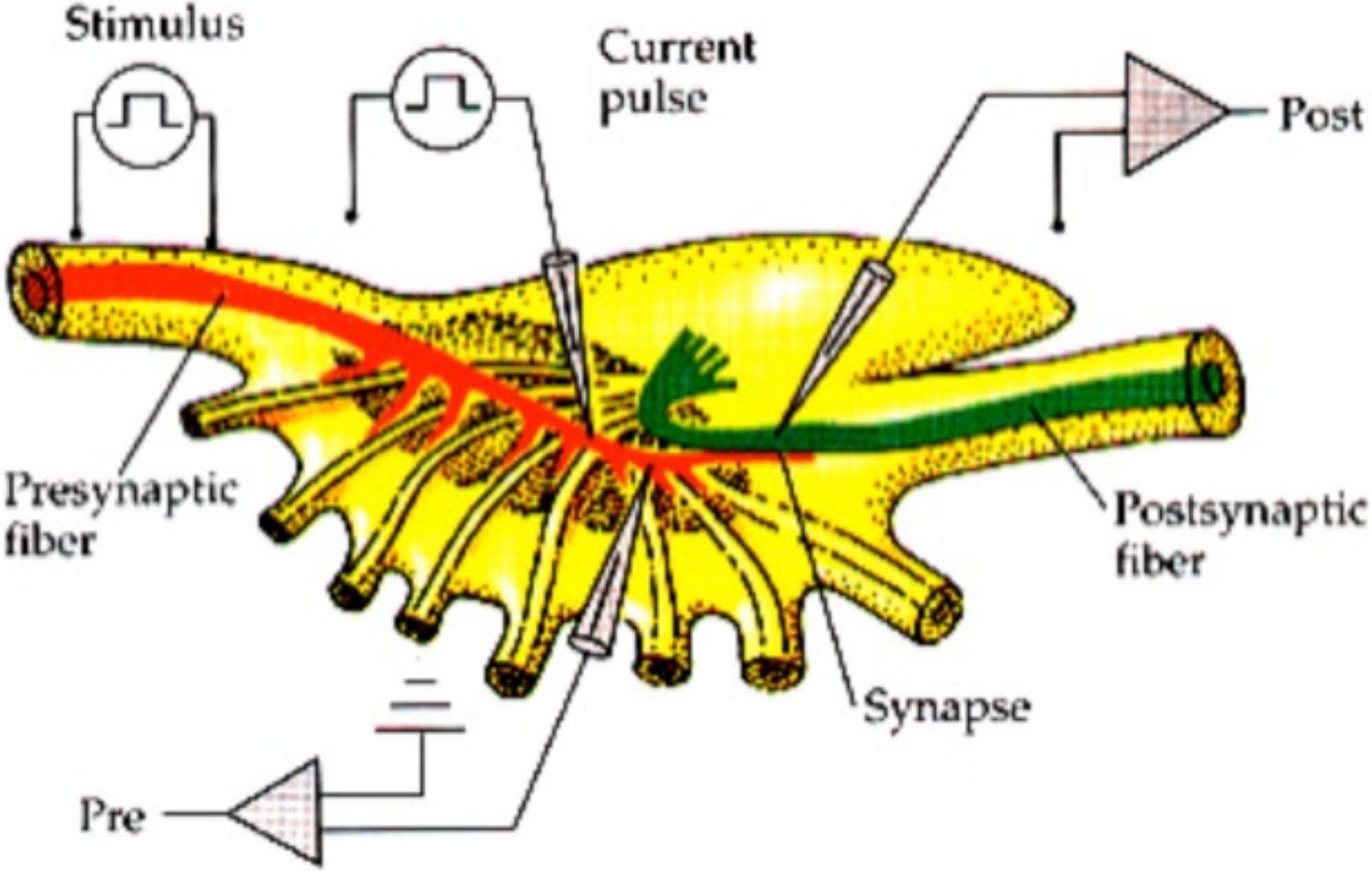

The transmitter release

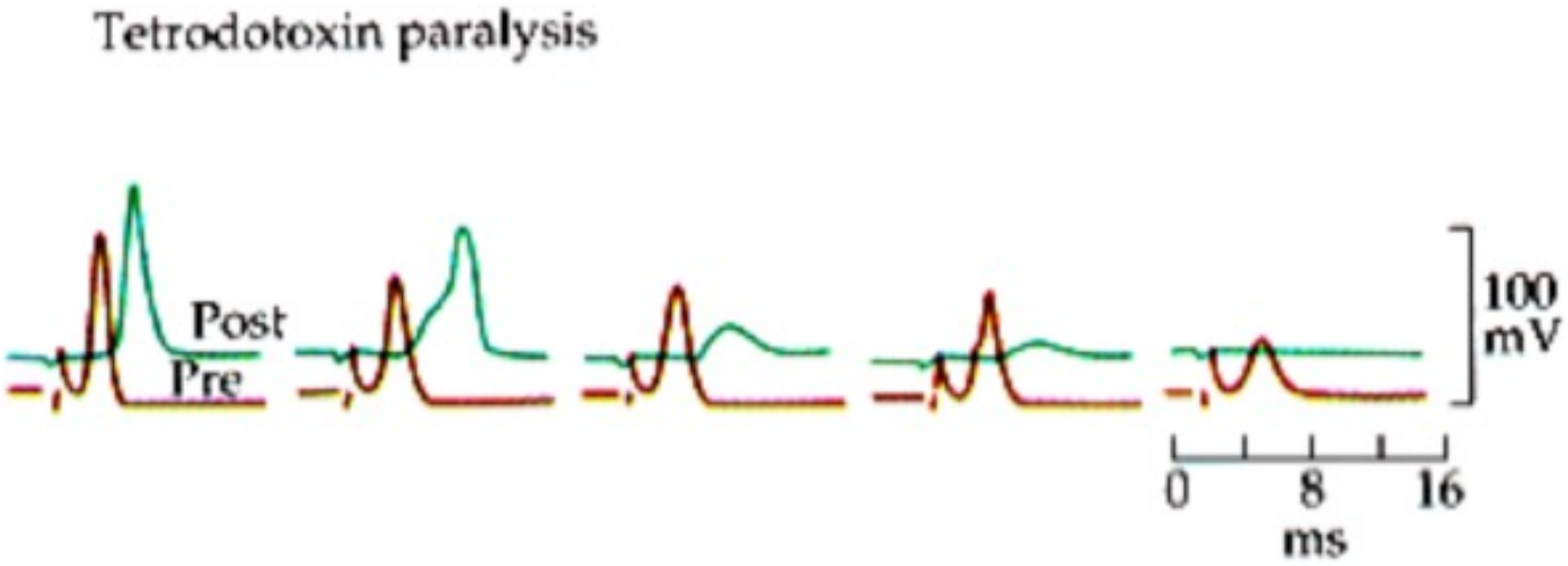

from Neuron to Brain

The synaptic delay

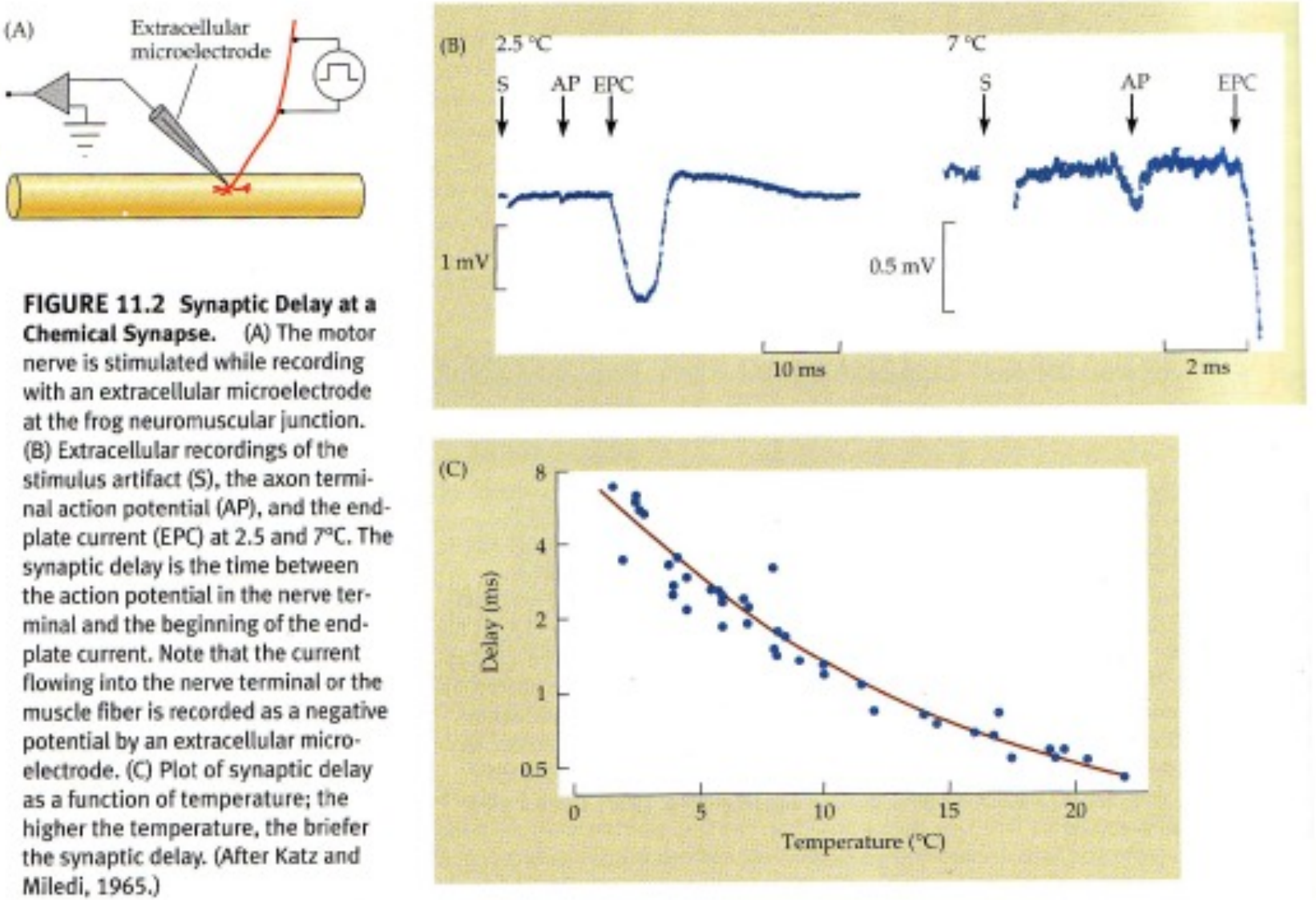

FIGURE 11.2 Synaptic Delay at a Chemical Synapse. (A) The motor nerve is stimulated while recording with an extracellular microelectrode at the frog neuromuscular junction. (B) Extracellular recordings of the stimulus artifact (S), the axon terminal action potential (AP), and the end-plate current (EPC) at 2.5 and 7°C. The synaptic delay is the time between the action potential in the nerve terminal and the beginning of the end-plate current. Note that the current flowing into the nerve terminal or the muscle fiber is recorded as a negative potential by an extracellular microelectrode. (C) Plot of synaptic delay as a function of temperature; the higher the temperature, the briefer the synaptic delay. (After Katz and Miledi, 1965.)

from Neuron to Brain

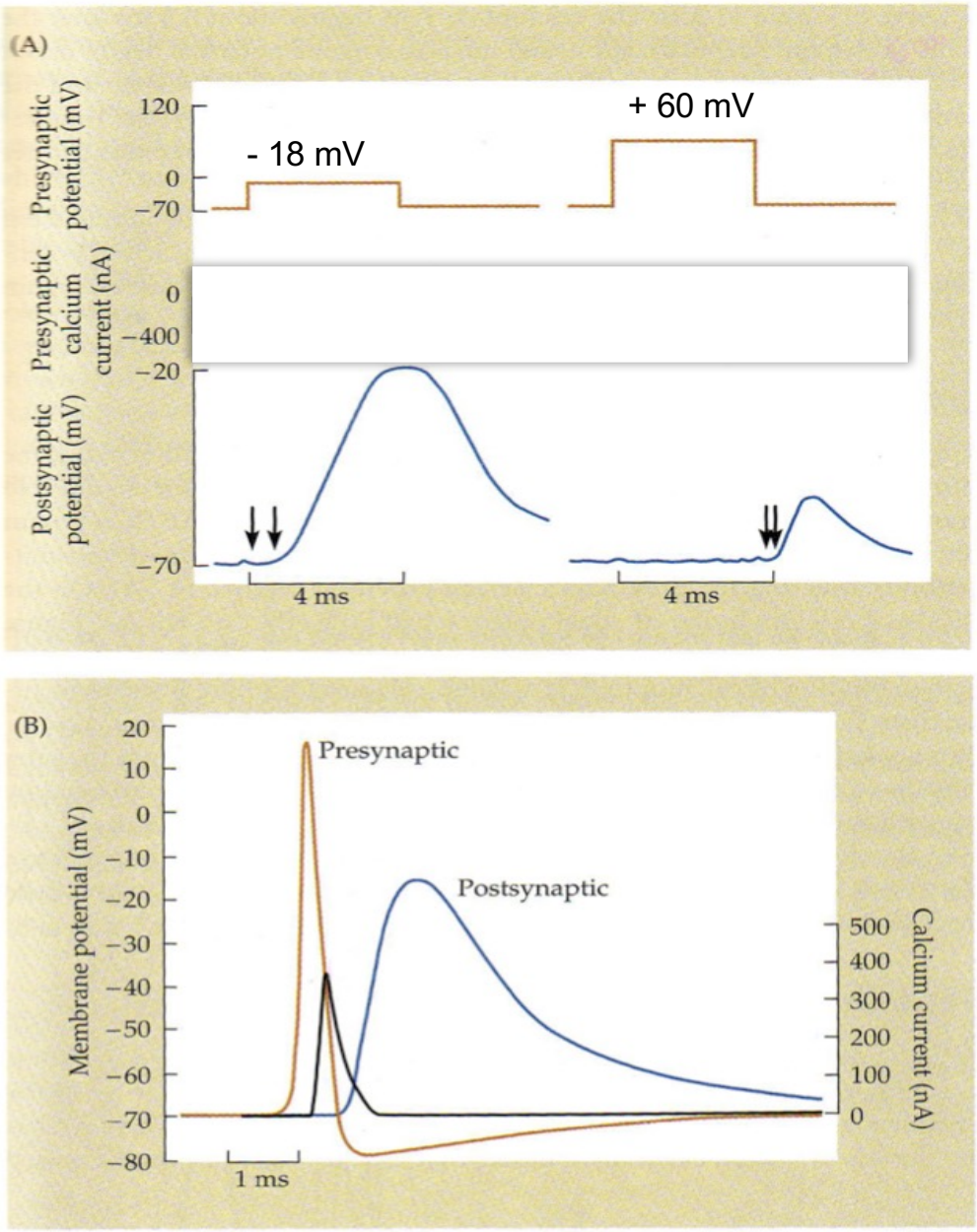

from Neuron to Brain

In which way can we block the synaptic release?

- By blocking the calcium channels
  - *Mg^{2+}, Cd^{2+}, Ni^{2+}, Mn^{2+} ....*
  - *Specific blockers*
- By blocking the presynaptic action potential
  - *TTX*
- Removing Ca^{2+} from the extracellular space

The events of the synaptic transmission

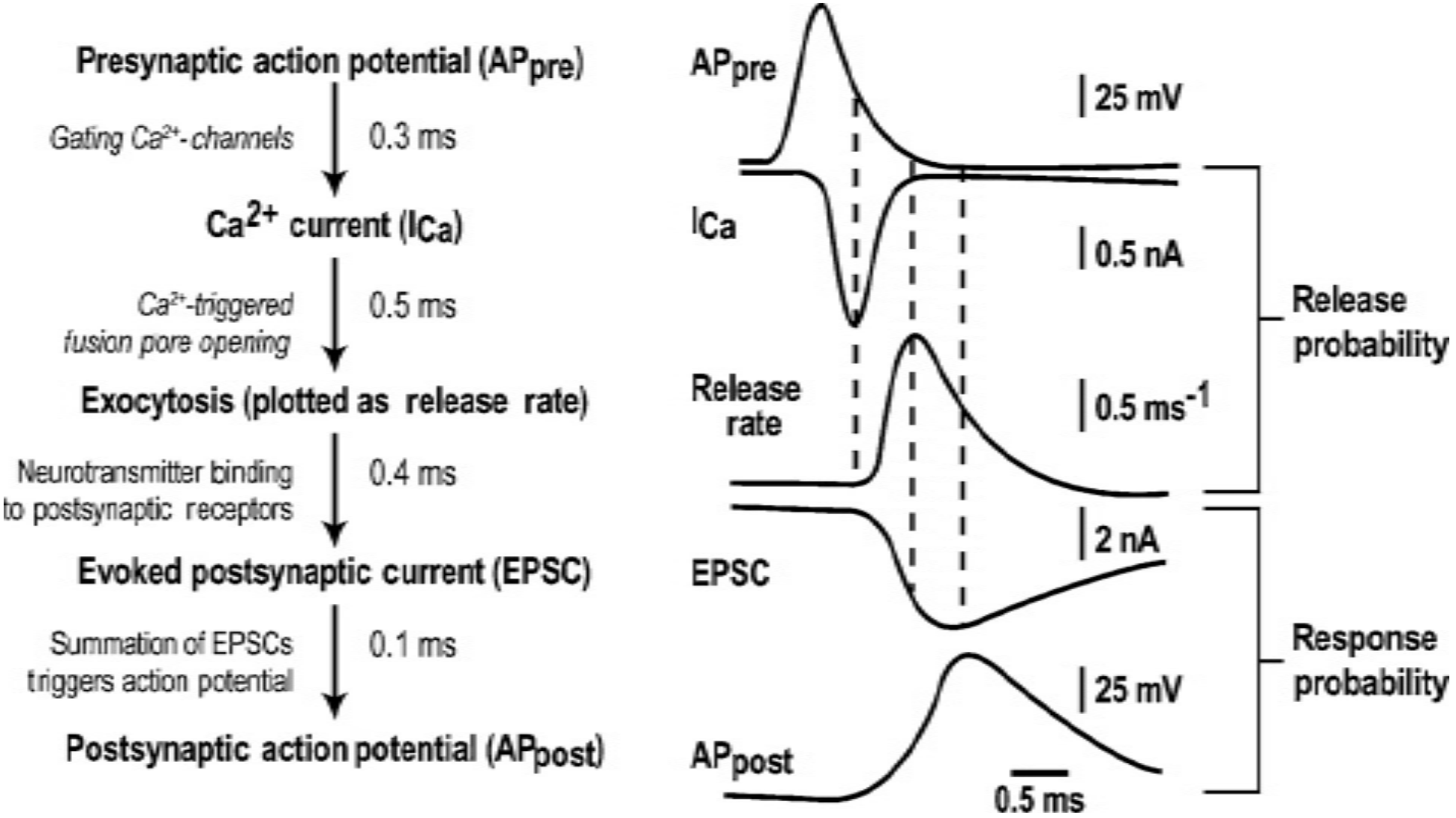

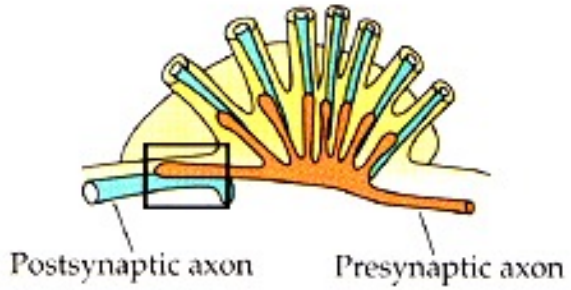

FIGURE 11.4 Microdomains of Calcium within the Presynaptic Terminal at the Squid Giant Synapse. (A) Distribution of calcium within the presynaptic axon terminal at rest, determined by intracellular injection of a calcium-sensitive dye (box in illustration at left shows the region imaged). (B) A brief train of presynaptic action potentials results in the appearance of microdomains of high calcium concentration within the axon terminal. (After Llinás, Sugimori, and Silver, 1992; micrographs kindly provided by R. Llinás.)

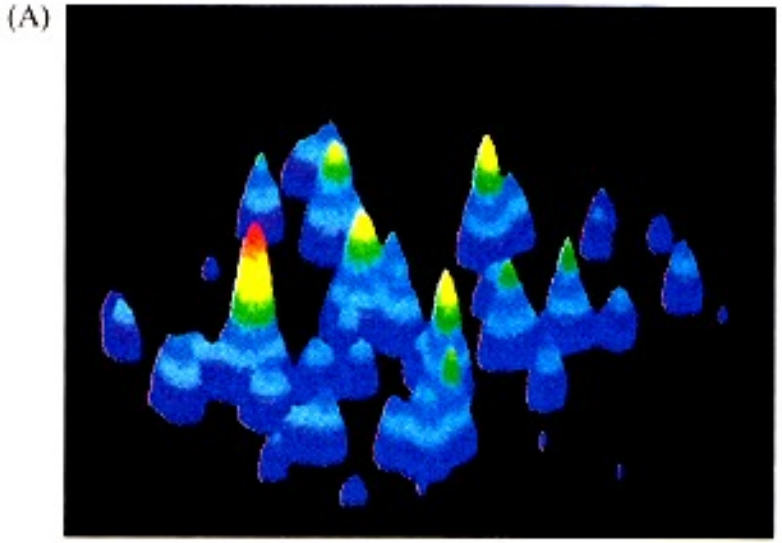

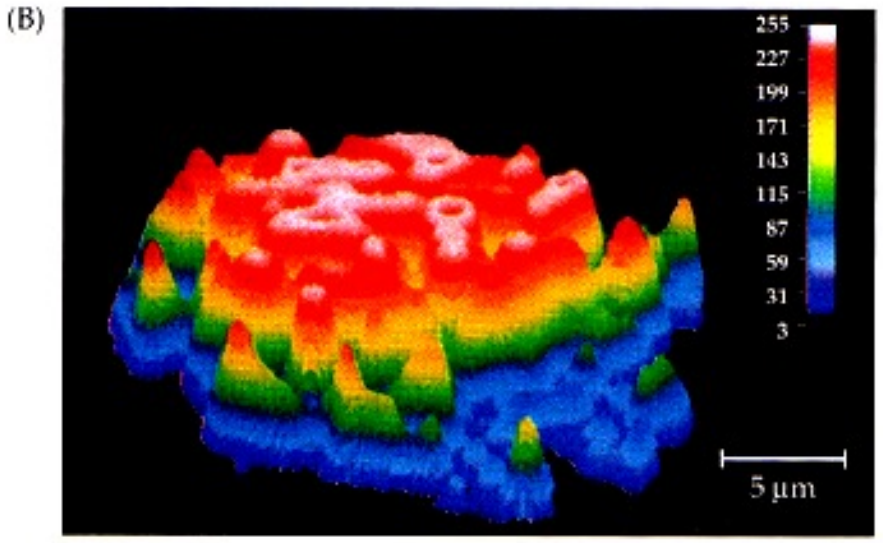

REST

Brief train of AP

from Neuron to Brain

FIGURE 11.5 Calcium Enters Near the Site of Transmitter Release at the squid giant synapse. (A) Intracellular recordings from the pre- and postsynaptic axons following injection of the fast calcium chelator BAPTA. Superimposed traces show the reduction in the EPSP during a 4 min BAPTA injection. (B) BAPTA binds calcium before it has time to reach the calcium sensor that triggers release. (C) Superimposed intracellular recordings during a 4 min injection of EGTA, a chelator that binds calcium more slowly. No change in EPSP amplitude is seen. (D) Calcium reaches the sensor that triggers release faster than it becomes bound to EGTA, indicating that the site of calcium entry must be within 100 nm of the site at which calcium triggers transmitter release. (A and C after Adler et al., 1991.)

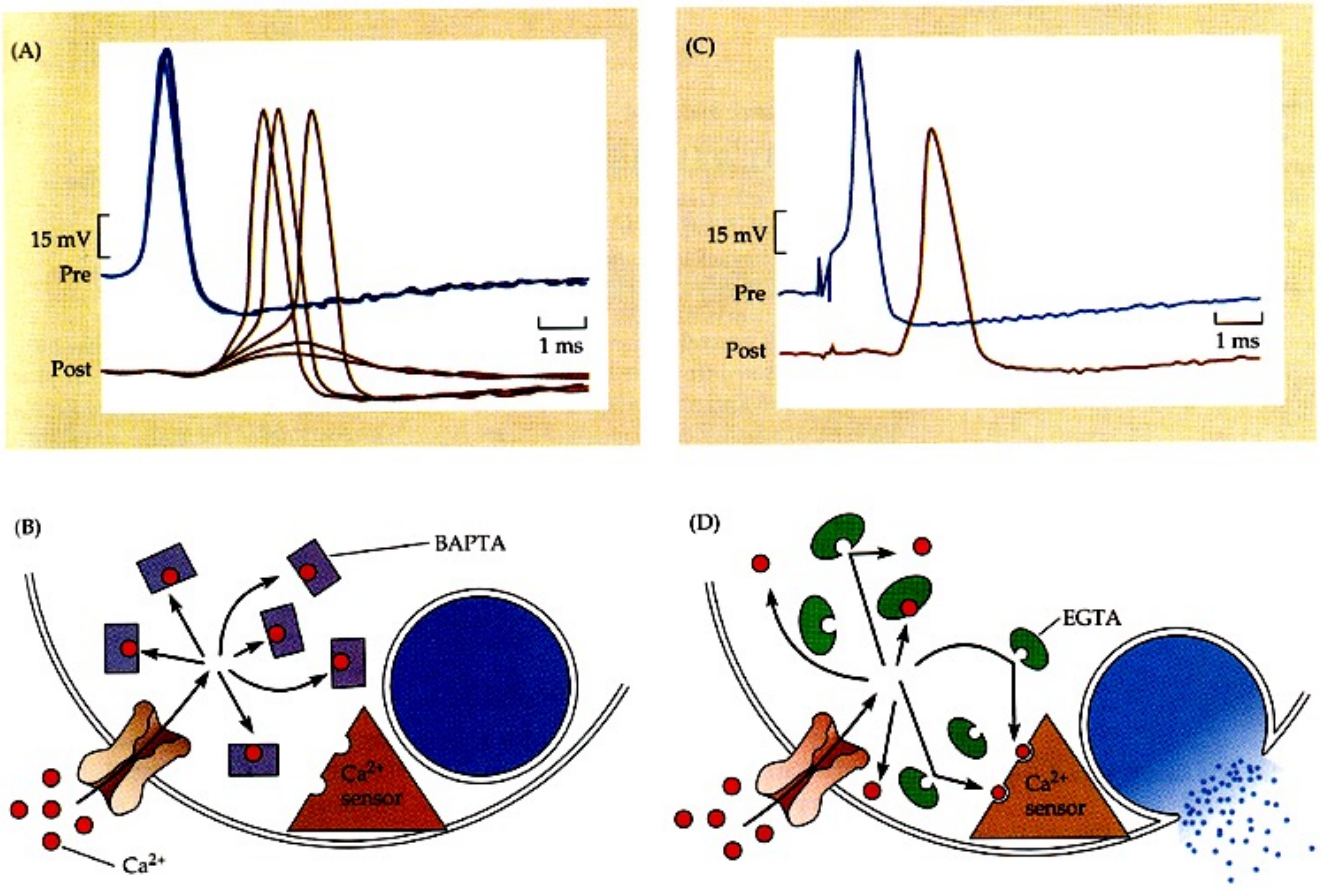

from Neuron to Brain

At rest

Endplate

Outside the endplate

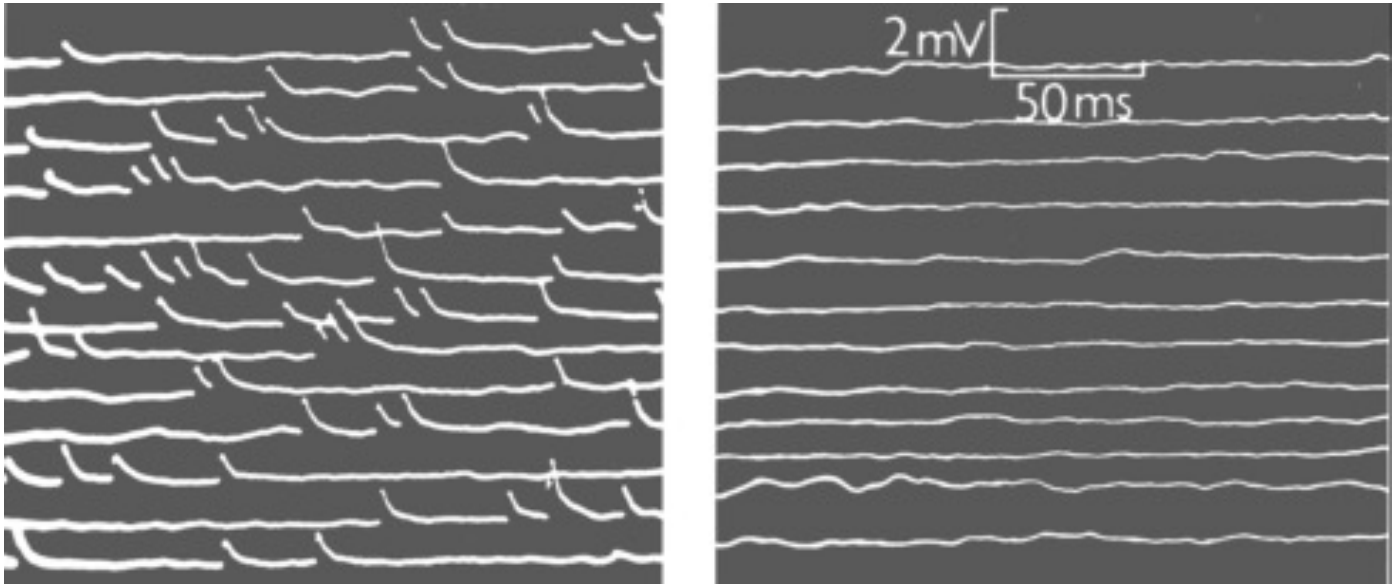

AP

Microelectrode at the endplate

Microelectrode far from the endplate

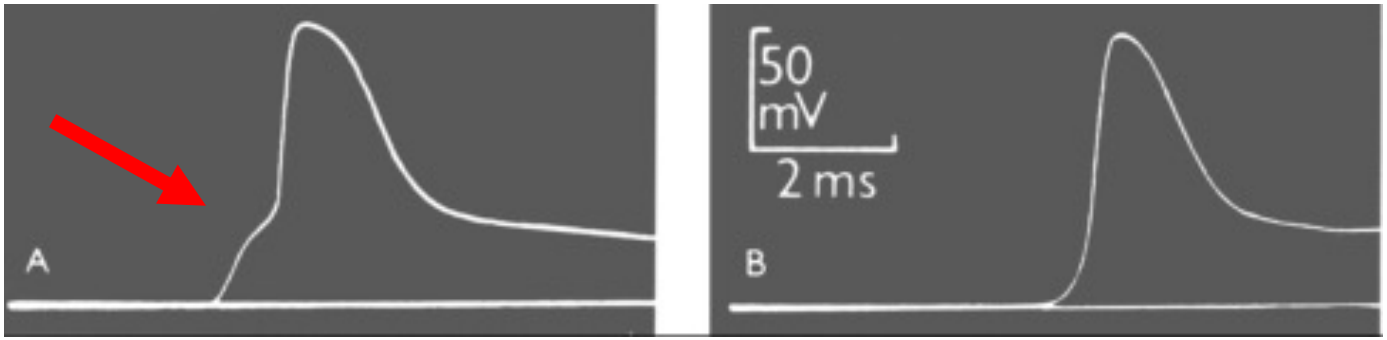

Intracellular recording from single muscle fibre of frog. (A) at the motor end-plate. Upper part shows spontaneous 'miniature end-plate potentials' which are localized at junction and arise from sudden discharge by motor nerve ending of packets of acetylcholine, each containing thousands of molecules. Lower part shows single response to nerve impulse which was started by electric shock at the beginning of trace; first step of response is large 'end-plate potential' resulting from synchronous delivery of few hundred packets of acetylcholine, this leading to full size action potential. (B) Traces recorded in same muscle fibre, 2mm away from end-plate. Upper part shows much attenuated and barely recognizable residues of miniature end-plate potentials. Lower part shows propagated action potential, delayed by conduction over 2 mm distance and not preceded by end-plate step. (From: P. Fatt and B. Katz, Nature, 166, 597 (1950)).

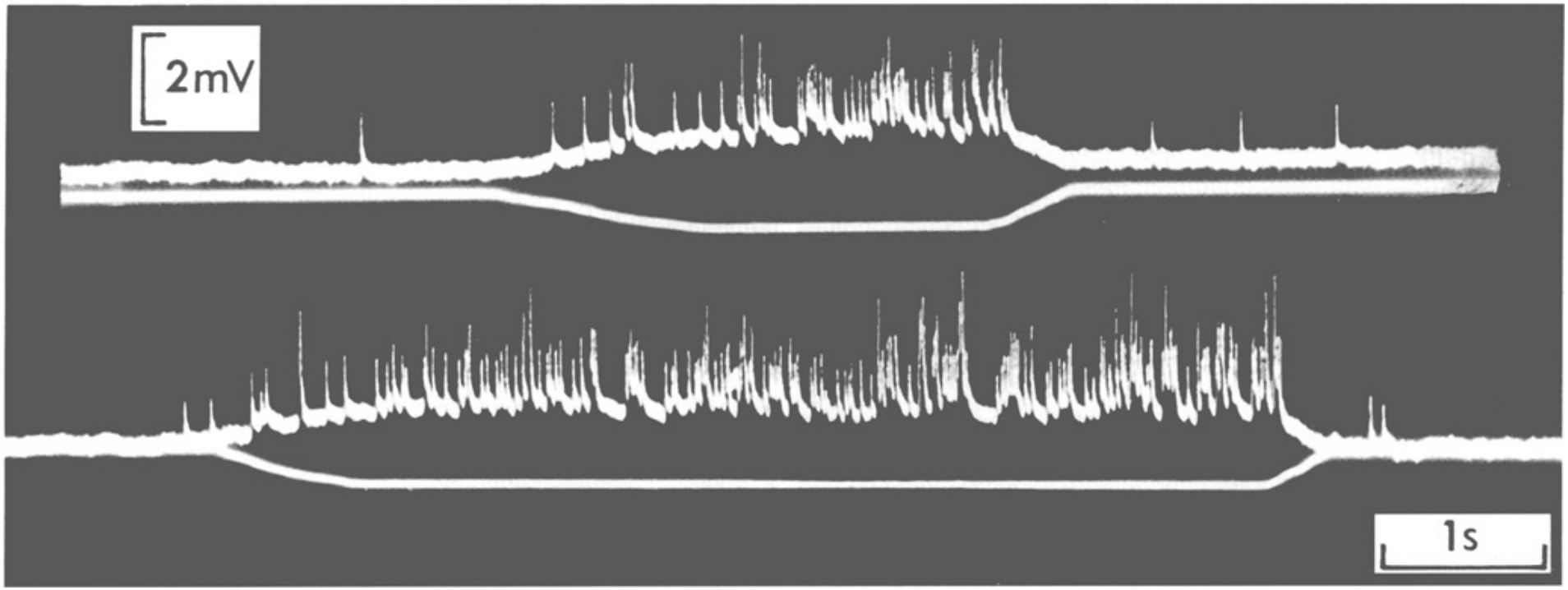

Presynaptic electrical control of the frequency of miniature end-plate potentials. In each pair of traces, the upper shows miniature potentials, the lower indicates current flowing through the terminal part of the motor axon. The cathode was placed near the junction so as to depolarize the nerve ending. See J. del Castillo and B. Katz, Journal of Physiology 124, 586 (1954).

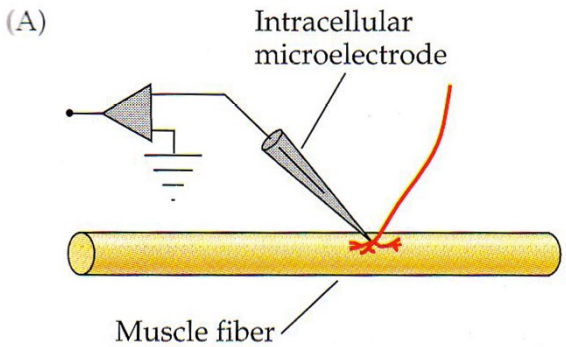

FIGURE 11.7 Miniature Synaptic Potentials occur spontaneously at the frog neuromuscular junction. (A) Intracellular recording from a muscle fiber in the region of the motor end plate. (B) Spontaneous miniature synaptic potentials are about 1 mV in amplitude and are confined to the end-plate region of the muscle fiber. (C) After addition of prostigmine, which prevents acetylcholinesterase from hydrolyzing ACh, miniature synaptic potentials are increased in amplitude and duration, but the frequency at which they occur is unchanged. This indicates that each miniature is due to a quantal packet of ACh, rather than to a single ACh molecule. (After Fatt and Katz, 1952.)

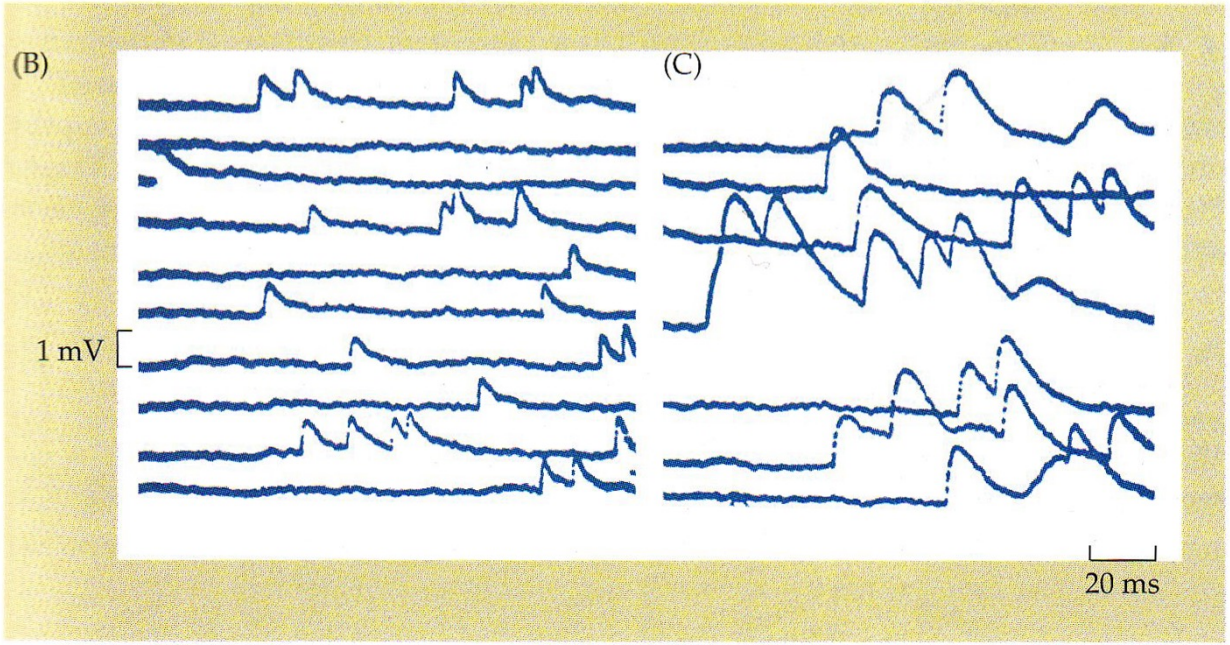

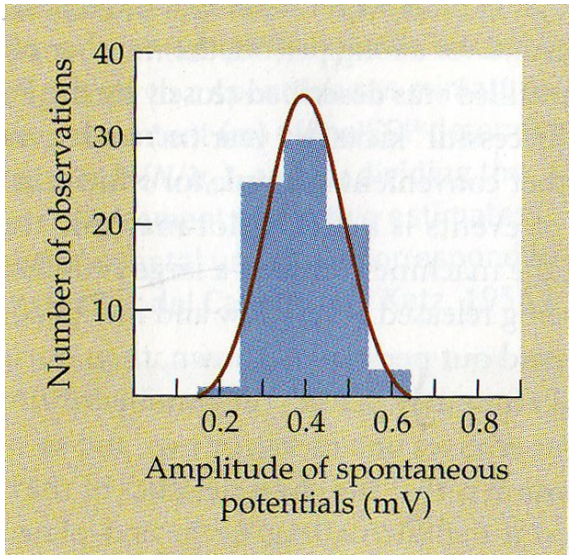

FIGURE 11.8 The End-Plate Potential Is Composed of Quantal Units That Correspond to Spontaneous Miniature Potentials. Presynaptic release of ACh at a frog neuromuscular junction was reduced by lowering the calcium concentration in the bathing solution. (A) Sets of intracellular records, each showing two to four superimposed responses to nerve stimulation. The amplitude of the end-plate potential (EPP) varies in a stepwise fashion; the smallest response corresponds in amplitude to a spontaneous miniature potential (MEPP). (B) Comparison of the mean quantal content (m) of the EPP determined in two ways: by applying the Poisson distribution, $m = \ln(N/n_0)$, and by dividing the mean EPP amplitude by the mean MEPP amplitude. Agreement of the two estimates supports the hypothesis that the EPP is composed of quantal units that correspond to spontaneous MEPPs. (A after Fatt and Katz, 1952; B after del Castillo and Katz, 1954.)

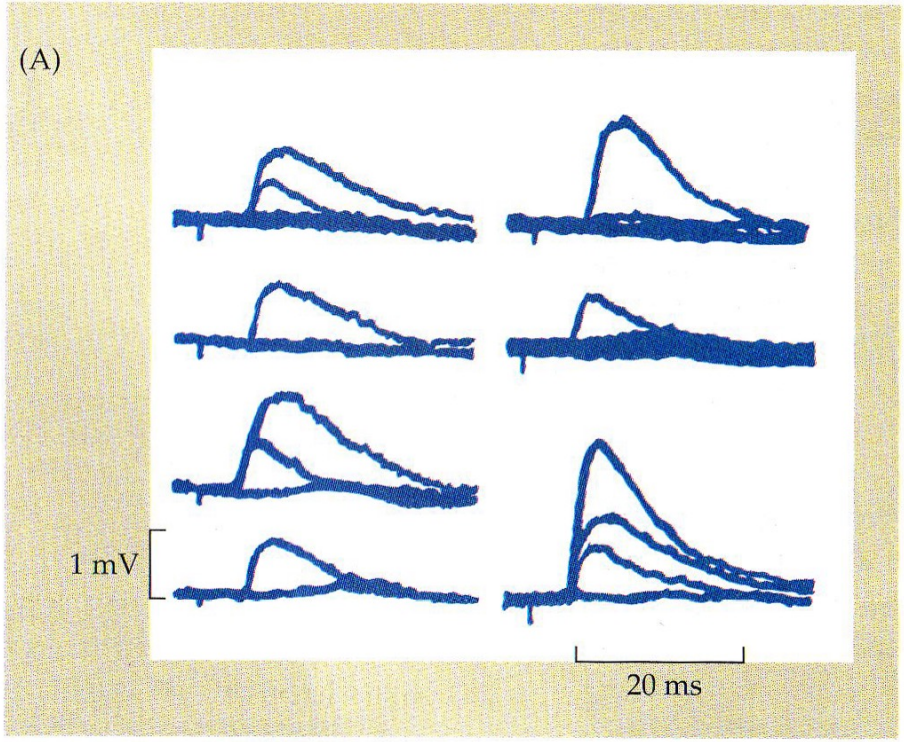

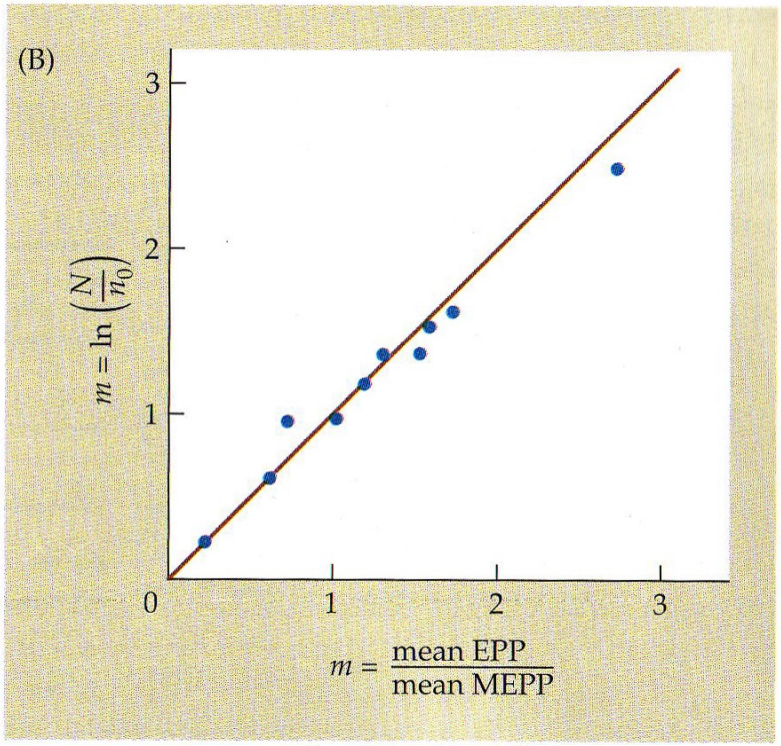

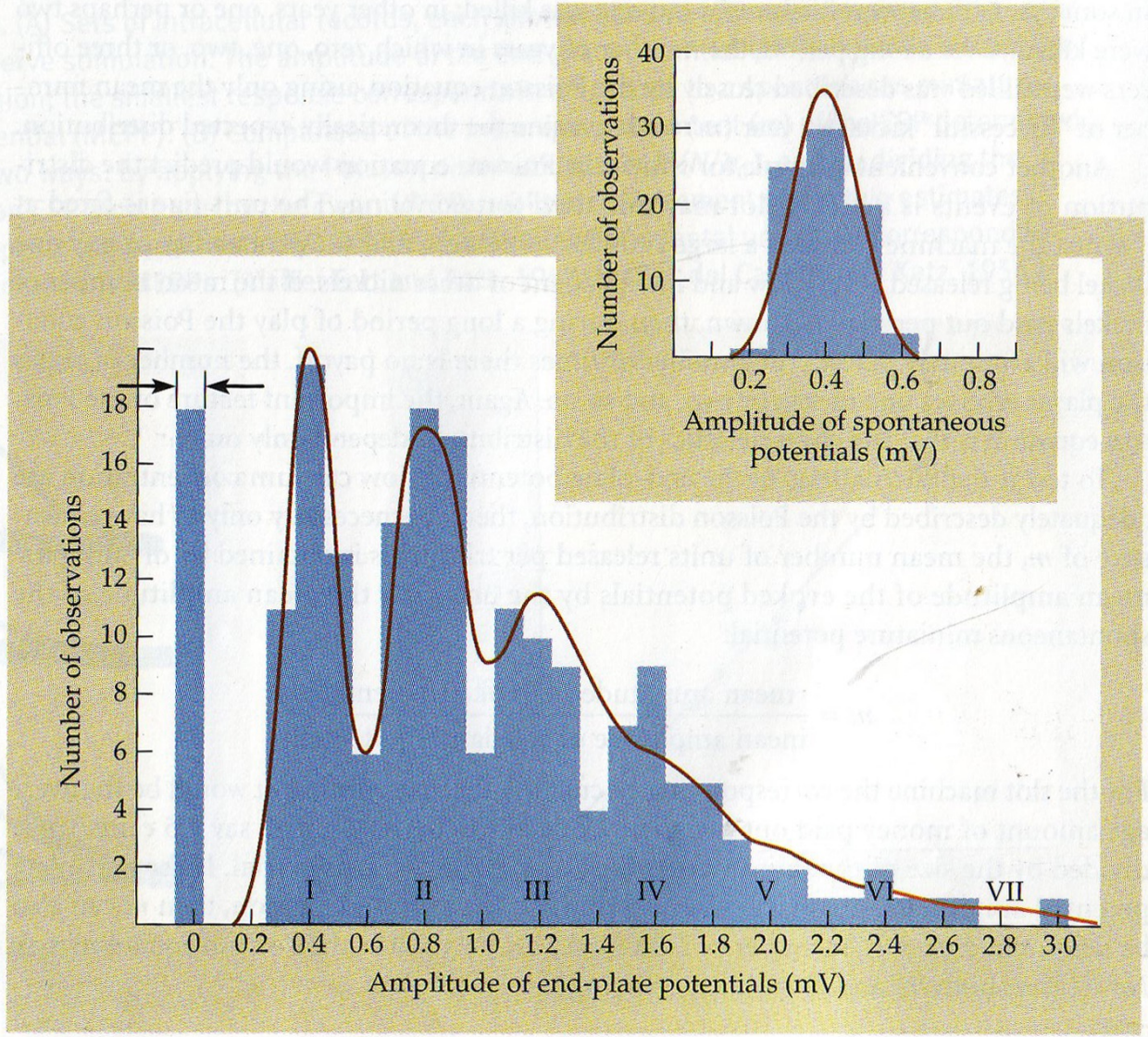

FIGURE 11.9 Amplitude Distribution of end-plate potentials at a mammalian neuromuscular junction in high (12.5 m*M*) magnesium solution. The histogram shows the number of end-plate potentials observed at each amplitude. The peaks of the histogram occur at 0 mV (failures) and at one, two, three, and four times the mean amplitude of the spontaneous miniature end-plate potentials (inset), indicating responses comprising 1, 2, 3, and 4 quanta. The solid line represents the theoretical distribution of end-plate potential amplitudes calculated according to the Poisson equation and allowing for the spread in amplitude of the quantal size. The arrows indicate the predicted number of failures. (From Boyd and Martin, 1956.)

FIGURE 11.10 The Number of ACh Molecules in a Quantum is determined by mimicking a spontaneous miniature end-plate potential with an ionophoretic pulse of ACh. (A) An intracellular microelectrode records spontaneous miniature end-plate potentials (MEPPs) and the response to ionophoretic application of ACh. (B) A MEPP is mimicked almost exactly by an ionophoretic pulse of ACh. The rate of rise of the ionophoretic ACh pulse is slightly slower because the ACh pipette is further from the postsynaptic membrane than is the nerve terminal. (B after Kuffler and Yoshikami, 1975a.)

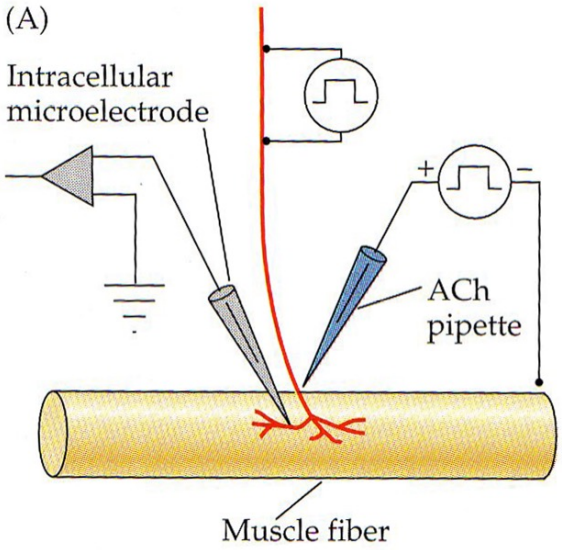

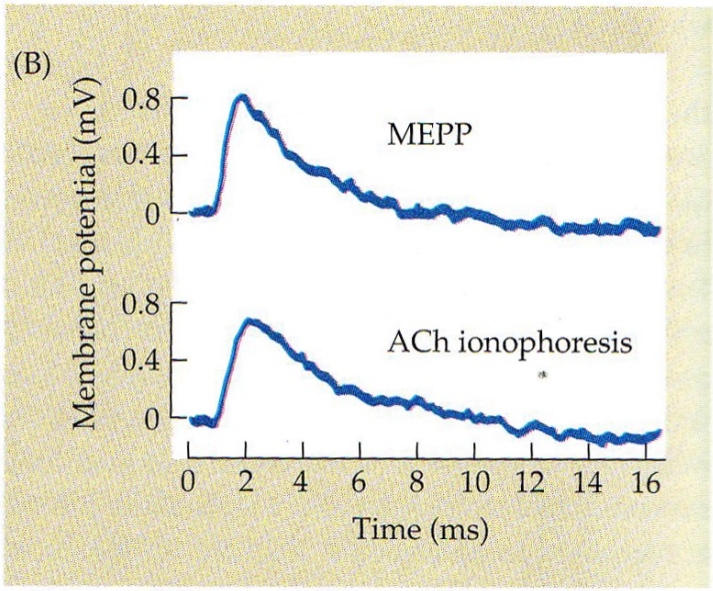

QUANTAL RELEASE

1 quantum corresponds to about 7000 ACh molecules

Quanta release means that only 0, 7000, 14000, or so on molecules will be released at the time

In general, the number of quanta released from the nerve terminal in response to AP (quantum content of a synaptic response) may vary considerably, but the number of molecules (quantum size) of each quantum is fixed.

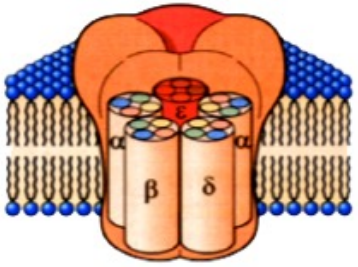

mEPP has a conductance of 40 nS

1 nAChR has a conductance of 30 pS

1300 open channels give a mEEP

(2600 ACh molecules)

The end-plate potential (EPP)

FIGURE 9.5 Synaptic Potentials recorded with an intracellular microelectrode from a mammalian neuromuscular junction treated with curare. The curare concentration in the bathing solution was adjusted so that the amplitude of the synaptic potential was near threshold and so on occasion evoked an action potential in the muscle fiber. (From Boyd and Martin, 1956.)

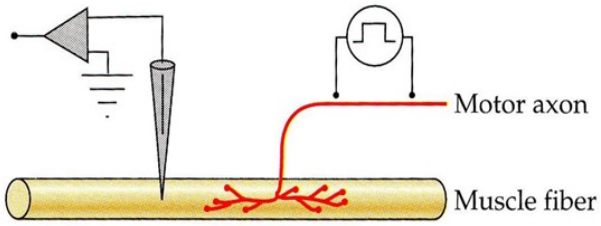

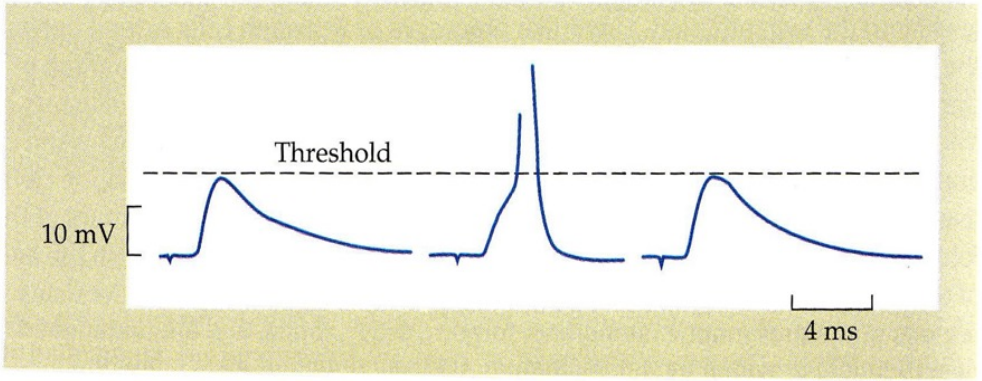

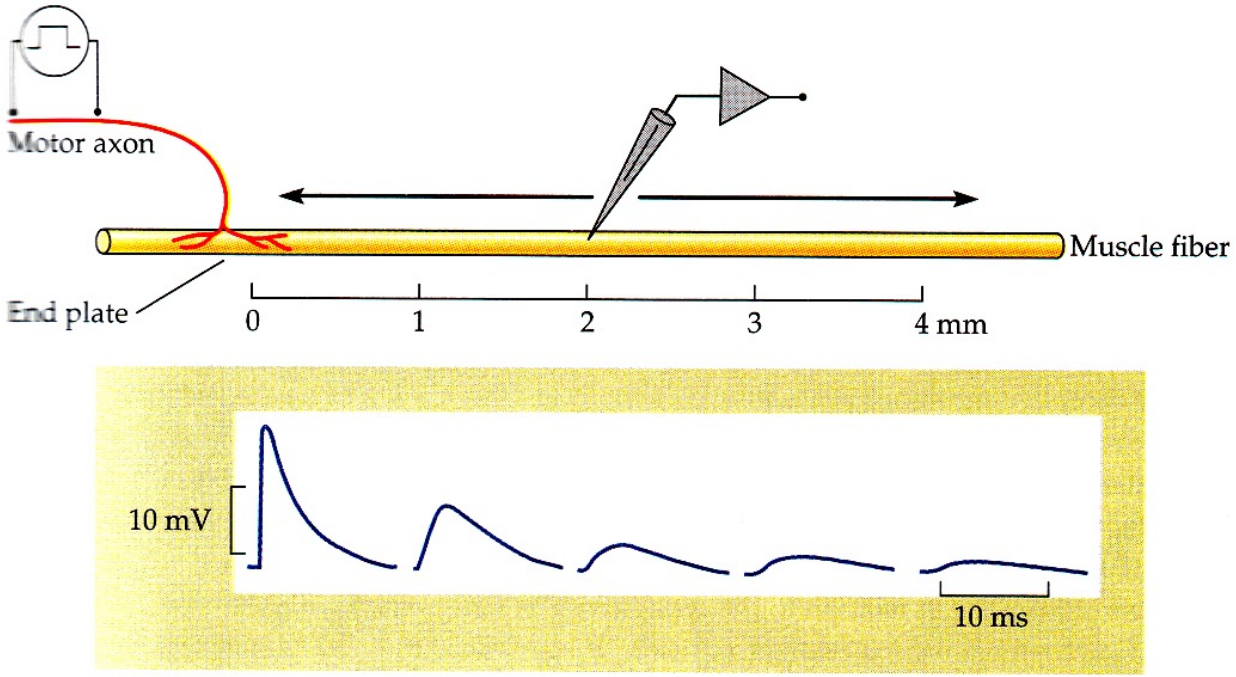

FIGURE 9.6 Decay of Synaptic Potentials with Distance from the end plate region of a muscle fiber. As the distance from the end plate increases, synaptic potentials recorded by an intracellular electrode decrease in size and rise more slowly. (After Fatt and Katz, 1951.)

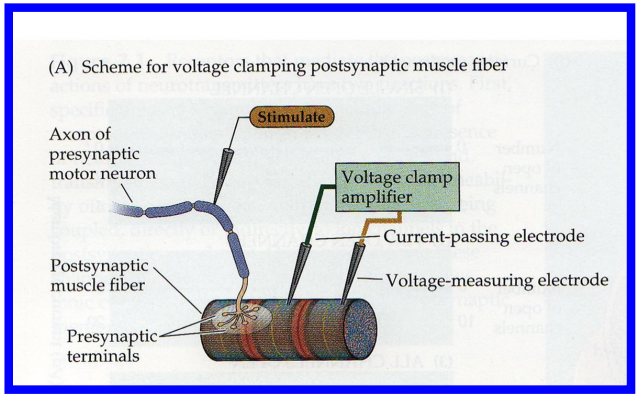

Figure 7.3 The influence of the postsynaptic membrane potential on end plate currents. (A) A postsynaptic muscle fiber is voltage clamped using two electrodes, while the presynaptic neuron is electrically stimulated to cause the release of ACh from presynaptic terminals. This experimental arrangement allows the recording of macroscopic EPCs produced by ACh. (B) Amplitude and time course of EPCs generated by stimulating the presynaptic motor neuron while the postsynaptic cell is voltage clamped at four different membrane potentials. (C) The relationship between the peak amplitude of EPCs and postsynaptic membrane potential is nearly linear, with a reversal potential (the voltage at which the direction of the current changes from inward to outward) close to 0 mV. Also indicated on this graph are the equilibrium potentials of Na^+, K^+, and Cl^- ions. (D) Lowering the external Na^+ concentration causes EPCs to reverse at more negative potentials. (E) Raising the external K^+ concentration makes the reversal potential more positive. (After Takeuchi and Takeuchi, 1960.)

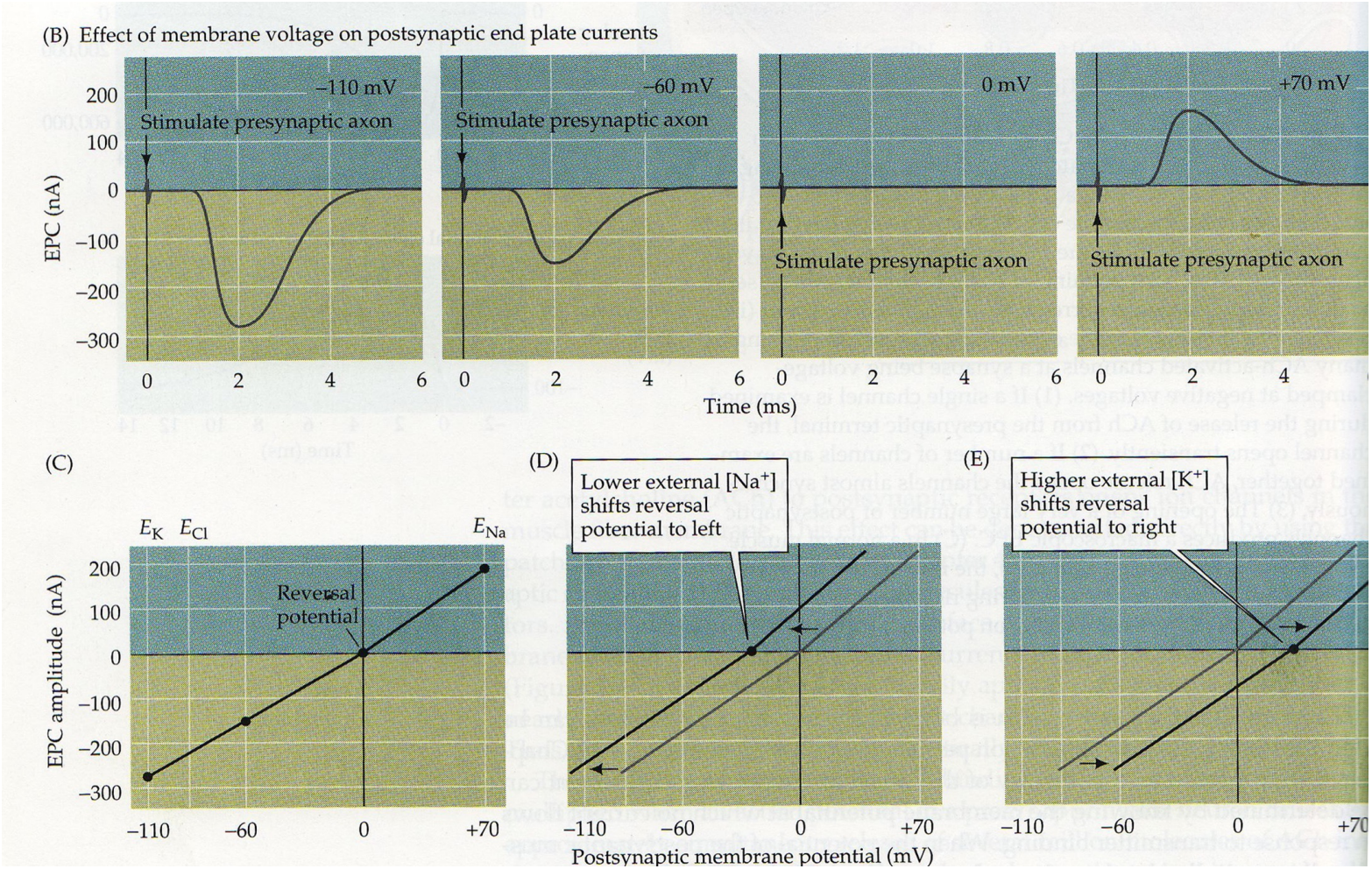

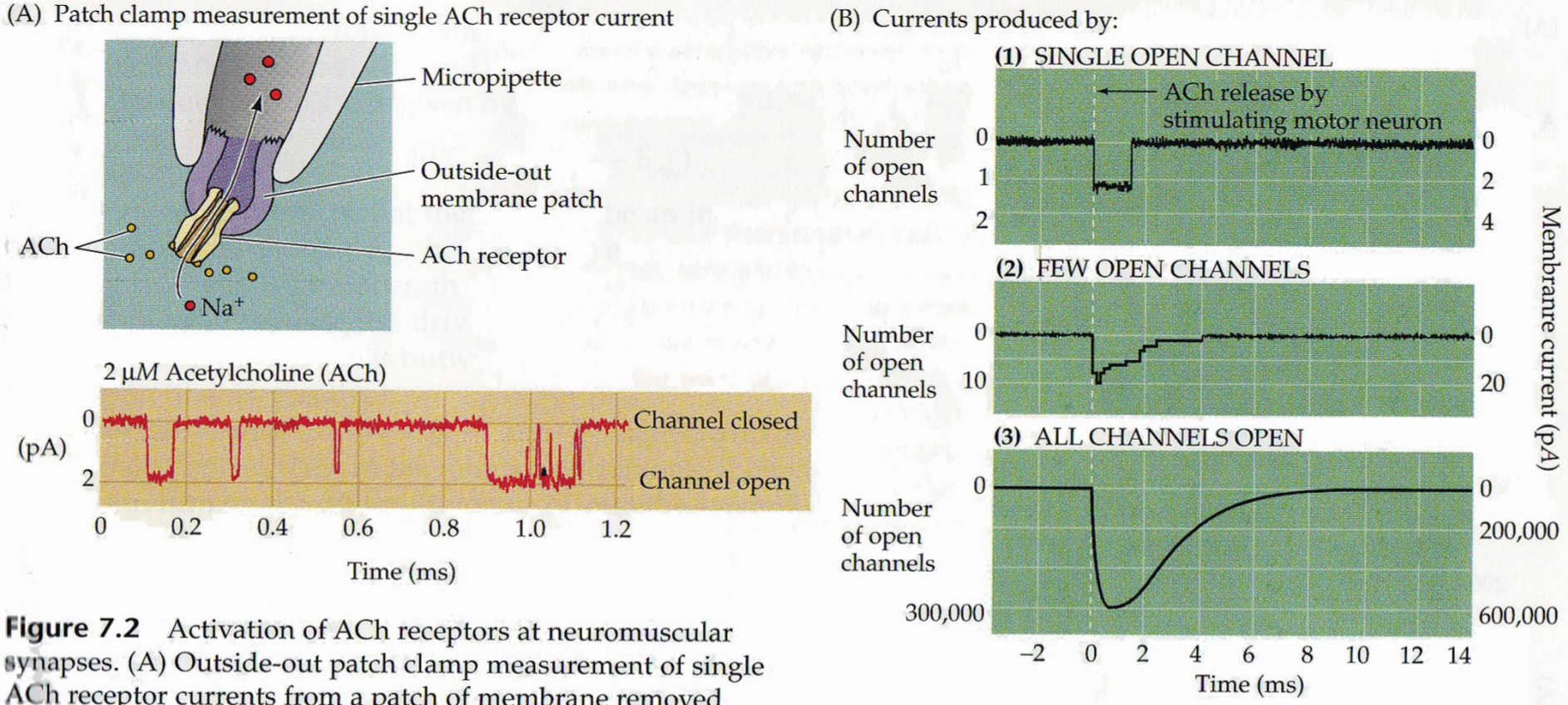

Figure 7.2 Activation of ACh receptors at neuromuscular synapses. (A) Outside-out patch clamp measurement of single ACh receptor currents from a patch of membrane removed from the postsynaptic muscle cell. When ACh is applied to the extracellular surface of the membrane clamped at negative voltages, the repeated brief opening of a single channel can be seen as downward deflections corresponding to inward current (i.e., positive ions flowing into the cell). (B) Synchronized opening of many ACh-activated channels at a synapse being voltage-clamped at negative voltages. (1) If a single channel is examined during the release of ACh from the presynaptic terminal, the channel opens transiently. (2) If a number of channels are examined together, ACh release opens the channels almost synchronously. (3) The opening of a very large number of postsynaptic channels produces a macroscopic EPC. (C) In a normal muscle cell (i.e., not being voltage-clamped), the inward EPC depolarizes the postsynaptic muscle cell, giving rise to an EPP. Typically, this depolarization generates an action potential (not shown).

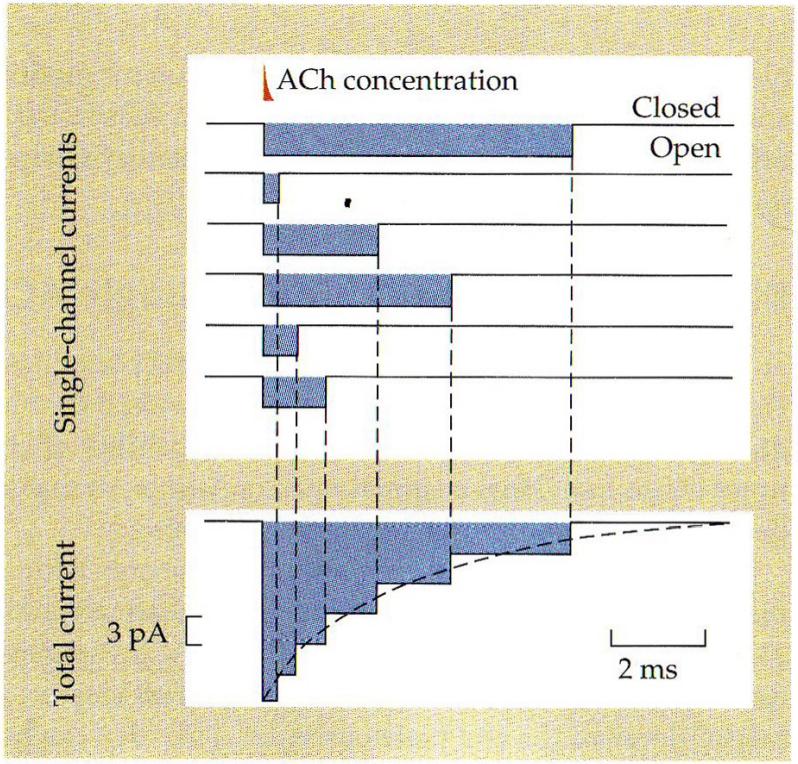

FIGURE 9.13 Total End Plate Current Is the Sum of Individual Channel Currents. Current flow through six individual channels is depicted in the top panel. Channels open instantaneously in response to ACh. ACh is rapidly hydrolyzed, preventing any further channel openings. Channel open times are distributed exponentially. The individual channel currents sum to give the total end plate current (lower panel). The time constant of the decay of the total current is equal to the mean open time of the individual channels.

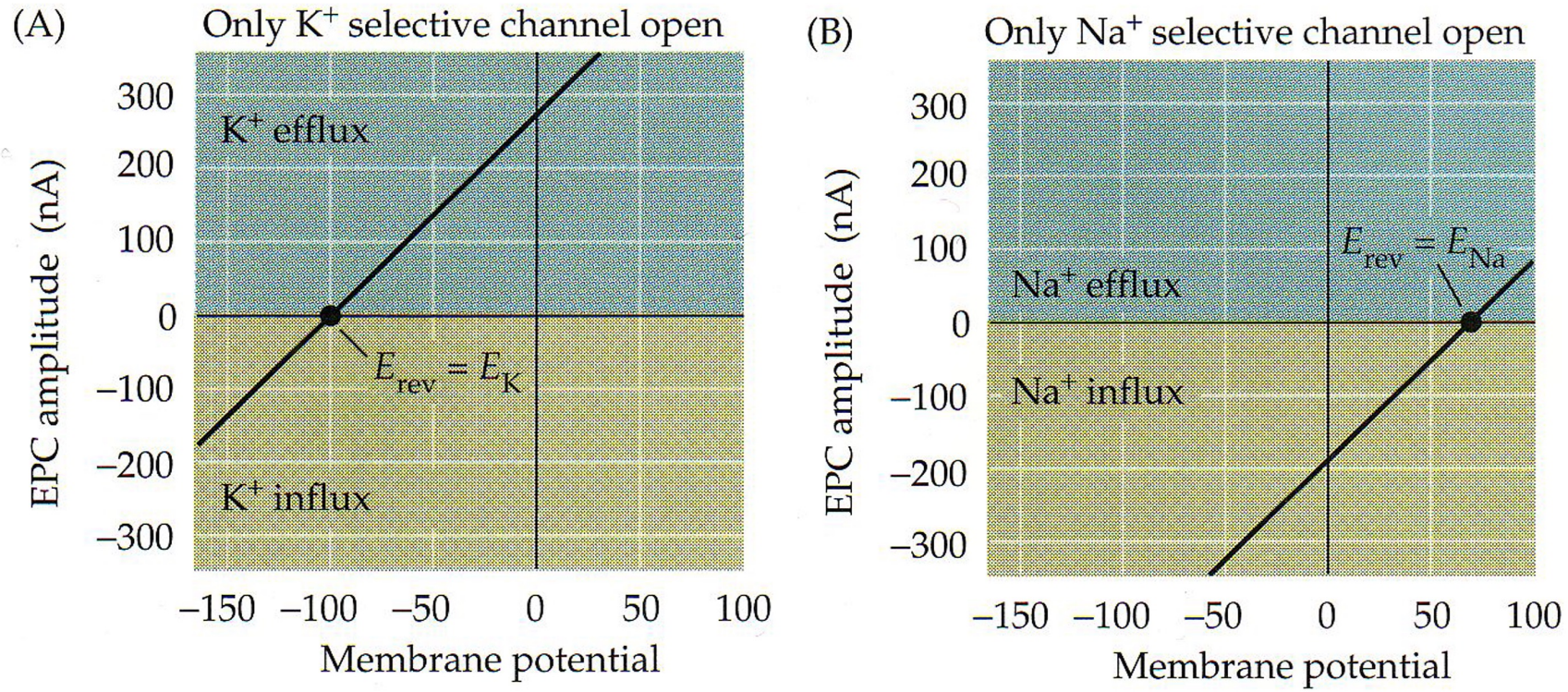
(A)
Only K+ selective channel open
K+ efflux
K+ influx
Erev = EK
EPC amplitude (nA)
300
200
100
0
–100
–200
–300
–150
–100
–50
0
50
100
Membrane potential
(B)
Only Na+ selective channel open
Na+ efflux
Na+ influx
Erev = ENa
EPC amplitude (nA)
300
200
100
0
–100
–200
–300
–150
–100
–50
0
50
100
Membrane potential

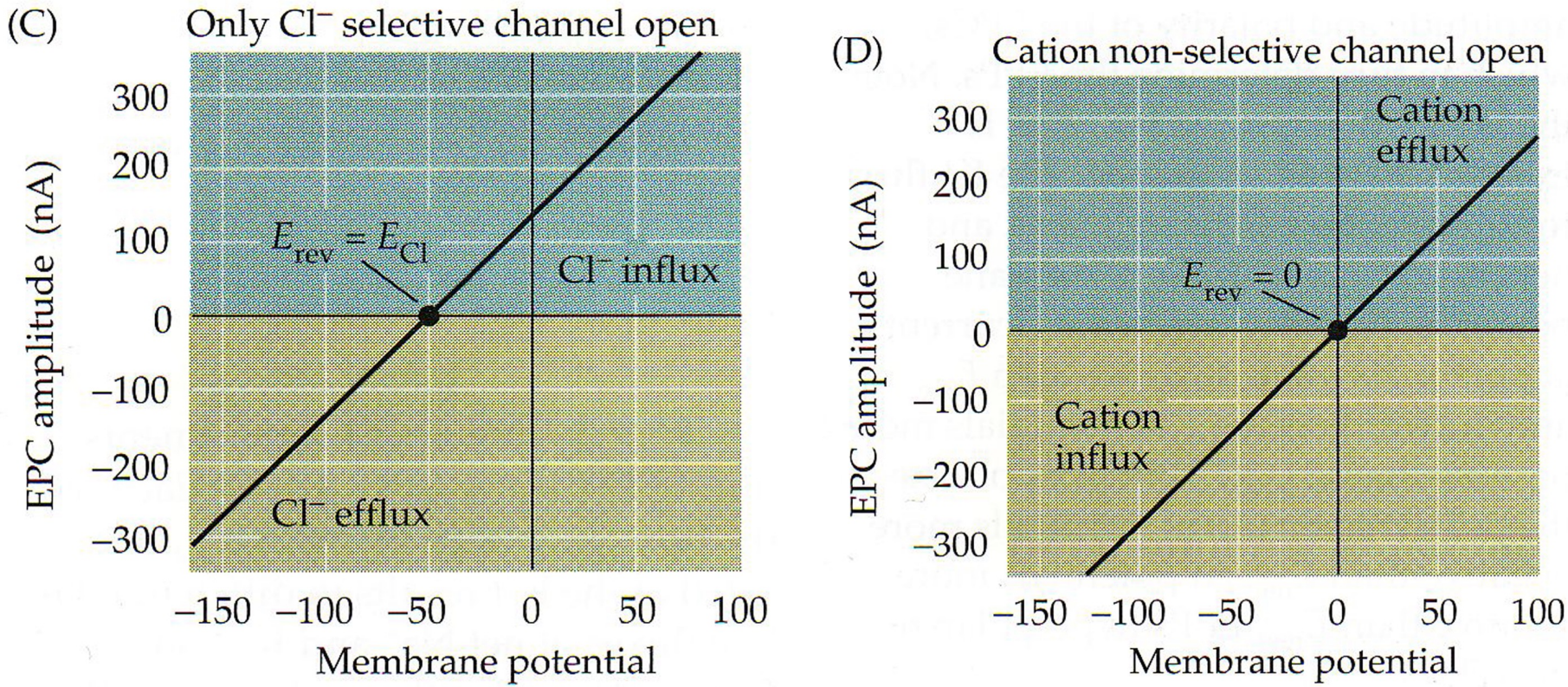

Figure 7.4 The effect of ion channel selectivity on the reversal potential. Voltage clamping a postsynaptic cell while activating presynaptic neurotransmitter release reveals the identity of the ions permeating the postsynaptic receptors being activated. (A) The activation of postsynaptic channels permeable only to K^+ results in currents reversing at E_K, near –100 mV. (B) The activation of postsynaptic Na^+ channels results in currents reversing at E_{Na}, near +70 mV. (C) Cl^- selective currents reverse at E_{Cl}, near –50 mV. (D) Ligand-gated channels that are about equally permeable to both K^+ and Na^+ show a reversal potential near 0 mV.

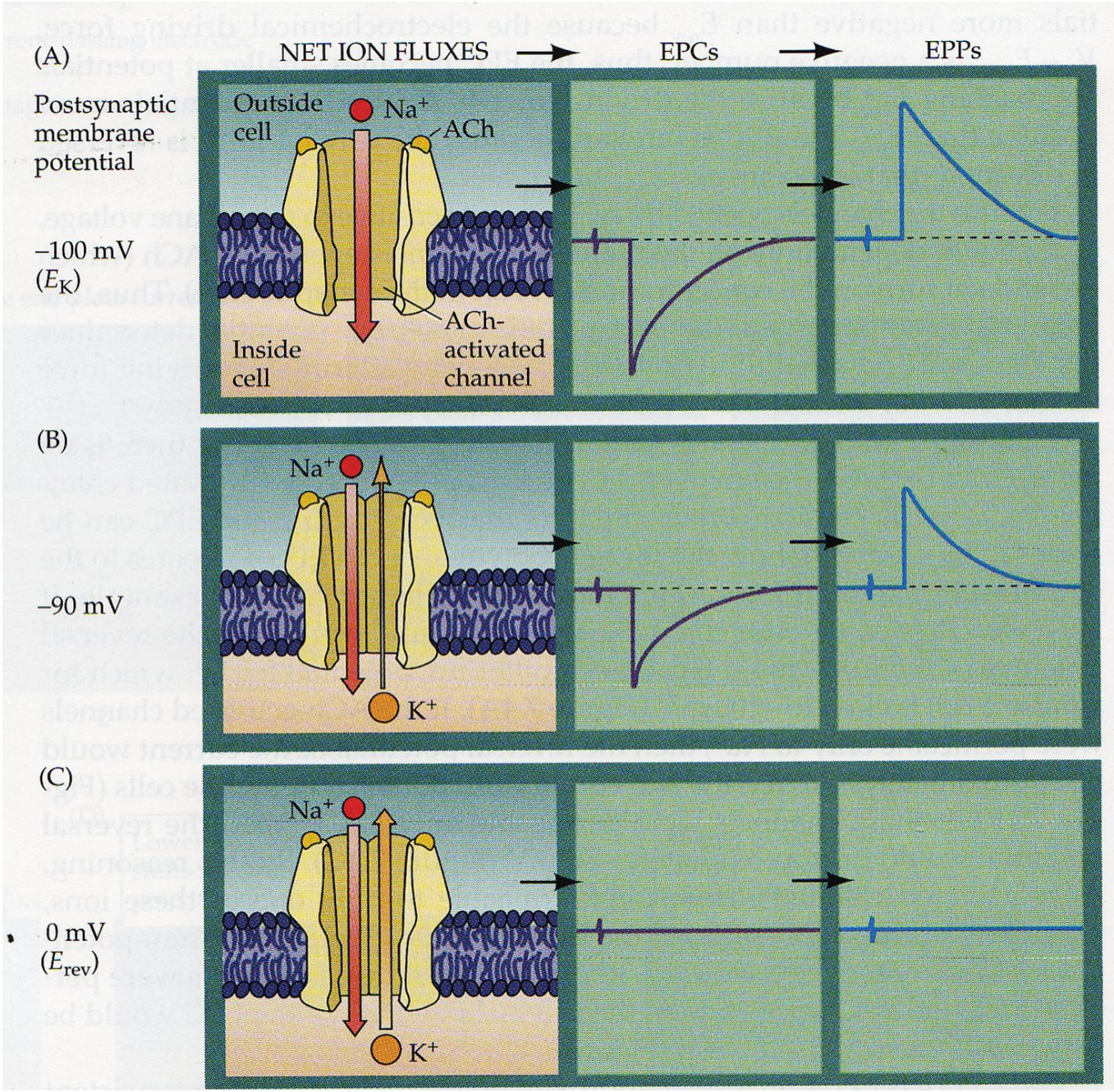

Figure 7.5 Na^+ and K^+ movements during EPCs and EPPs. (A–D) Each of the postsynaptic potentials (V_{post}) indicated at the left results in different relative fluxes of net Na^+ and K^+ (ion fluxes). These ion fluxes determine the amplitude and polarity of the EPCs, which in turn determine the EPPs. Note that at about 0 mV the Na^+ flux is exactly balanced by an opposite K^+ flux resulting in no net current flow, and hence, no change in the membrane potential. (E) EPCs are inward currents at potentials more negative than E_{rev} and outward currents at potentials more positive than E_{rev}. (F) EPPs depolarize the postsynaptic cell at potentials more negative than E_{rev}. At potentials more positive than E_{rev}, EPPs hyperpolarize the cell.

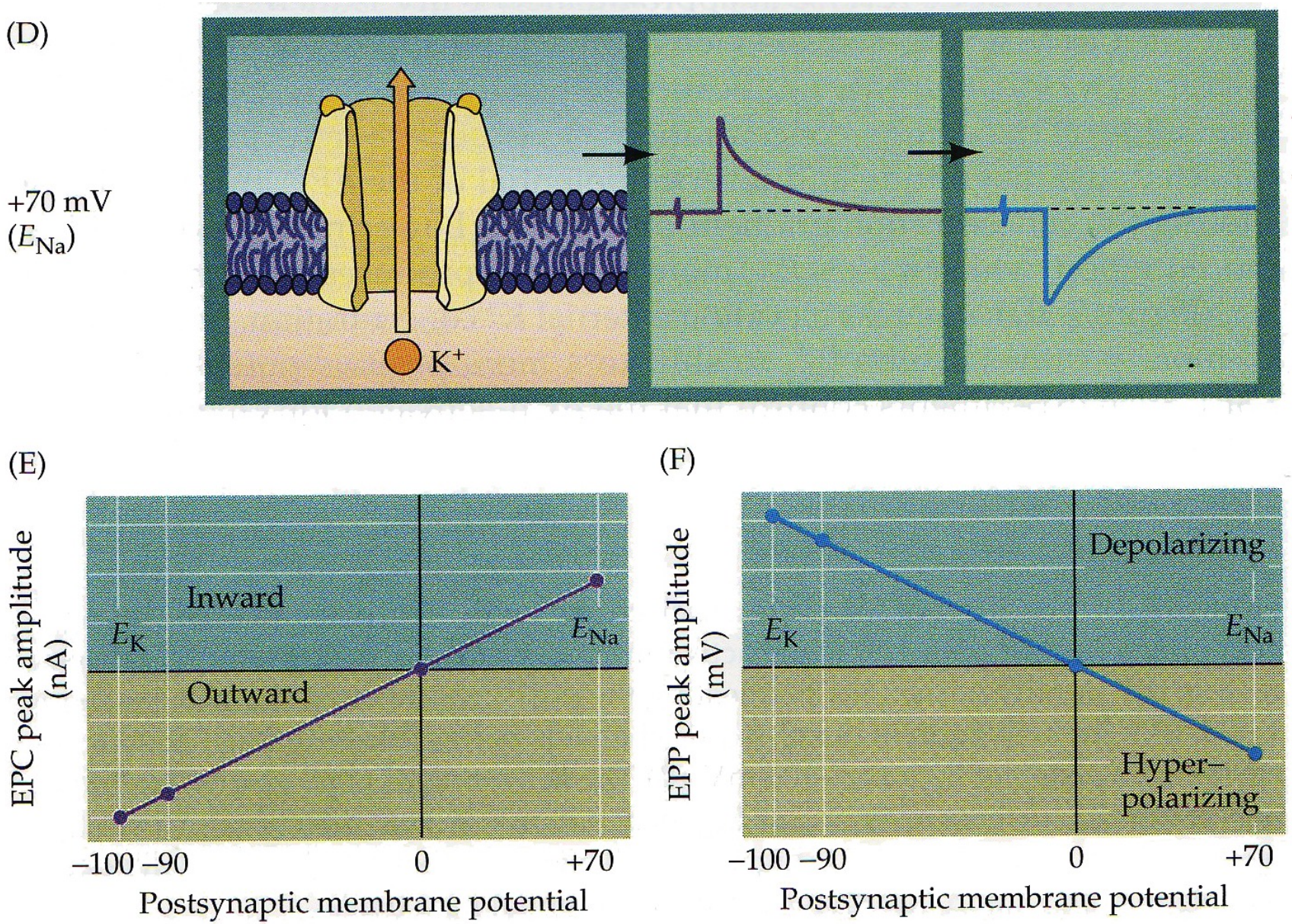
(D)
+70 mV
(E_{Na})
K^+
(E)
EPC peak amplitude
(nA)
Inward
Outward
E_K
E_{Na}
–100 –90
0
+70
Postsynaptic membrane potential
(F)
EPP peak amplitude
(mV)
Depolarizing
Hyper–
polarizing
E_K
E_{Na}
–100 –90
0
+70
Postsynaptic membrane potential

Video